Journal of Functional Materials and Applied Engineering

Research Paper

Molecular weight-controllable regenerated cellulose nanocrystal for Pickering emulsion application

Alejandro Vargas[1], Erik Johansen[1], Fattma Fischer[2,*]

[1] Suleman Dawood School of Business, Lahore University of Management Sciences, Lahore, Pakistan
[2] Department of Biological Sciences, King Abdul-Aziz University, Jeddah, Saudi Arabia
*Corresponding author: Alejandro.Vargas@lums.edu.pk; Johansen@lums.edu.pk; FaFische@yahoo.com

Abstract. Employing an aqueous NaOH/urea solvent and absolute ethanol as the anti-solvent, regenerated cellulose nanocrystals (RCNC) were fractionated via a multi-step precipitation protocol to yield populations with tunable molecular weights and sequentially reduced yet uniform particle dimensions. Chromatographic and electron-microscopy analyses confirmed that RCNC dimensions scaled inversely with molecular weight across the 36–9 kDa range. Pickering emulsion assays revealed pronounced surfactant-like behaviour for all fractions; the 15 kDa specimen (RCNC-15) outperformed the rest, generating the finest droplet sizes and maintaining maximal stability even at minimal loadings. When this optimal RCNC fraction was employed as a scaffold for in-situ nucleation of zinc oxide nanoparticles, the resulting hybrid catalysed the photodegradation of Nile red within an emulsion medium, attaining 99.5 % decomposition in 100 min and establishing RCNCs as high-efficiency carriers for emulsion-assisted catalytic processes.

Keywords: *regenerated cellulose nanocrystal; Pickering emulsion; high stability; photo degradation*

Received on 02 April 2025, Accepted on 25 April 2025, Published on 11 June 2025

1 Introduction

Cellulose is a linear, high-molecular-weight biopolymer built from repeating D-glucopyranose units joined via β-1,4-glycosidic linkages; neighbouring chains are held together by a network of hydrogen bonds and van der Waals interactions. Using currently common top-down treatment methods (such as mechanical method (ball milling[3]), acid hydrolysis[4-5] or enzymatic treatment[6]), needle-like cellulose nanocrystals (CNC) or fibrous cellulose nanofibers (CNF) can be obtained, both of which are collectively called cellulose nanomaterials[7]. Another bottom-up method for preparing cellulose nanomaterials is to precipitate dissolved cellulose molecules (chains) by using an anti-solvent to obtain regenerated cellulose (RC). Since cellulose is essentially insoluble in water and most organic solvents[8], a large number of studies have been devoted to developing simple and efficient solvents (such as pre-cooled alkali/urea/water system[9]) to dissolve as much cellulose as possible conveniently, and to inhibit cellulose dissolution by forming competitive hydrogen bonds between anti-solvents (such as water, ethanol, acetone, etc.) and cellulose molecules (chains), so that the dissolved cellulose precipitates and reorganizes from the solution to obtain regenerated cellulose nanocrystals (RCNC)[10-11].

Due to considerations of biosafety and environmental protection, cellulose-based materials have been widely used to stabilize Pickering emulsions (an emulsion system discovered by Ramsden[12] and Pickering[13] that uses colloidal particles instead of surfactants). Since the efficiency of Pickering emulsion stabilizers is closely related to their size, morphology, etc.[14], and most RCNC are prepared by one-time anti-solvent precipitation, the obtained RCNC usually has a wide molecular weight distribution, and the size and morphology are difficult to control, which is not conducive to stabilizing Pickering emulsions.

In this study, NaOH/urea/water solvent system was used, and a multi-step precipitation method was adopted to achieve controllable preparation of RCNC with different molecular weights and sizes. The obtained RCNC was used as a Pickering emulsion stabilizer, and the relationship between the molecular weight and size of RCNC and

its emulsifying performance was investigated. Furthermore, ZnO nanoparticles were grown in situ on the surface of RCNC with relatively optimal emulsifying performance, and the potential of the obtained RCNC as an emulsion-assisted reaction carrier was verified by an emulsion-assisted photo-degradation test of Nile red model reaction.

2 Experimental methods

2.1 Preparation of RCNC

Initially, 5 g of microcrystalline cellulose was dispersed in 200 mL of a ternary solvent system comprising anhydrous ethanol, ethylene glycol, and 1.2 N hydrochloric acid at a mass ratio of 1:1:1, followed by refluxing at 90 °C for 10 h. Upon completion of the reflux period, the resulting solid was isolated and subjected to three successive centrifugation-washing cycles with deionized water. Subsequently, the purified precipitate was transferred into a pre-chilled aqueous solution (200 mL) containing 5 % NaOH and 5 % urea, where it was mechanically agitated at −12 °C until full dissolution was achieved. Thereafter, under continuous stirring, 40 mL of absolute ethanol was introduced dropwise into the cellulose solution, inducing the precipitation of regenerated cellulose nanocrystals (RCNC). The precipitated material was then recovered by centrifugation and rinsed repeatedly with anhydrous ethanol until a neutral pH was attained, yielding sample 1#. Subsequently, under stirring, another 40 mL anhydrous ethanol was added dropwise to the supernatant after centrifugation of sample 1# in the previous step, and the obtained precipitate was collected by centrifugation and washed with anhydrous ethanol until neutral to obtain sample 2#. By repeating the above process repeatedly, samples 3#, 4#, 5#, and 6# were obtained respectively. The molecular weights of 1# to 6# RCNC samples gradually decreased from 36 kDa to 9 kDa. According to the molecular weight, the obtained RCNC were named: RCNC-36, RCNC-25, RCNC-15, RCNC-11, RCNC-10, and RCNC-9.

2.2 Preparation of oil-in-water Pickering emulsion

The as-synthesised RCNC was deployed as a particulate stabiliser to formulate oil-in-water (O/W) Pickering emulsions, with n-hexadecane comprising the dispersed phase and water constituting the continuous medium. First, RCNC was dried at 25 °C until anhydrous ethanol completely evaporated to avoid the influence of anhydrous ethanol on emulsion performance. Subsequently, RCNC was dispersed in 50 mmol/L NaCl aqueous solution to prepare uniform RCNC aqueous suspensions with concentrations of 0.5, 1.0, 2.0, 4.0 g/L. Then, 1.5 mL n-hexadecane was added to 6 mL uniformly dispersed RCNC suspension (50 mmol/L NaCl) to obtain an oil/water mixture with a volume ratio of 1:4. Finally, an ultrasonic instrument (UP-250) equipped with a 3 mm diameter titanium probe was used to ultrasonically prepare RCNC-stabilized O/W Pickering emulsion: the probe was placed about 3 mm below the liquid surface, and ultrasonicated at 50% output power for 25 s in a working mode of 2 s ultrasound followed by 3 s standby, to obtain a milky opaque RCNC-stabilized O/W Pickering emulsion. The oil/water volume ratio of all emulsions in this work was 1:4.

2.3 Preparation of ZnO@RCNC composite

RCNC-15 served as the scaffold template. It was first dispersed in a mixed-acid medium comprising 90 % 3 mol L^{-1} citric acid and 10 % 6 mol L^{-1} HCl at a solid-to-liquid ratio of 1:50 (m/v), then thermostated in an 80 °C water bath for 6 h under constant agitation. Afterward, the mixture was rapidly quenched to ambient temperature and the pH was brought to neutrality using 3 mol L^{-1} $NH_3 \cdot H_2O$. The resulting neutral suspension was partitioned into three equal aliquots, to which 0.1 mol L^{-1} $Zn(NO_3)_2 \cdot 6H_2O$ was introduced at mass ratios of 1:2, 2:2 and 3:2, respectively. Each aliquot was re-neutralised with 0.5 mol L^{-1} NaOH. Subsequently, under continued stirring at 80 °C, an equivalent volume of 0.1 mol L^{-1} NaOH was introduced into each portion to precipitate Zn^{2+} as $Zn(OH)_2$. The solids were then recovered by centrifugation, washed three times with de-ionised water, and air-dried at 25 °C. A final thermal treatment at 120 °C for 1 h converted the zinc hydroxide into ZnO, affording in-situ ZnO-decorated RCNC-15 denoted as ZnO@RCNC-15_x:2 (x = 1, 2, 3).

2.4 Molecular weight characterization

Molecular-weight distributions of the RCNC fractions were determined by gel-permeation chromatography (HPLC, LC-20AT) at a column temperature of 80 °C. Poly(ethylene glycol) standards of known molecular weight were used for calibration. Each RCNC sample was dissolved in 8 % LiCl/DMAc; 10 µL aliquots were injected and eluted with 0.5 % LiCl/DMAc at 1 mL min^{-1}. The dispersity index (Đ) was computed as the ratio of weight-average to number-average molecular weight (Đ = M_w/M_n).

2.5 Size characterization

Transmission electron microscopy (TEM, Tecnai F20) was used to characterize the size of the obtained RCNC. The obtained RCNC samples were dispersed in anhydrous ethanol at a ratio of 0.005% respectively and ultrasonicated for 10 min to disperse RCNC uniformly. Then, about 50 µL of the dispersion was sucked with a pipette and dropped on a copper grid covered with a carbon support film. Before dropping the sample, the grid was cleaned with plasma (Fischione 1020) for 3 s to avoid RCNC agglomeration during evaporation of anhydrous ethanol. Finally, TEM with an acceleration voltage of 200 kV was used to characterize the size of the obtained samples. Since cellulose-based materials are electron beam sensitive materials with low critical electron dose, they are prone to radiation damage during TEM characterization[15]. Therefore, during TEM characterization, to avoid high-energy electron beam radiation damage as much as possible, the spot size mode was set to 5 to reduce the radiation electron dose. All sample TEM characterizations were performed no less than 10 times.

2.6 Fluorescence staining characterization

(1) Nile red (NR) staining of n-hexadecane. First, 10 mg NR was dissolved in 10 mL acetone in the dark to prepare 1 mg/mL NR staining solution. Subsequently, 200 µL of 1 g/L RCNC-stabilized Pickering emulsion was dispersed in 2 mL 50 mmol/L NaCl aqueous solution. Then, 20 µL NR staining solution was dropped into the obtained dispersion, and allowed to stand in the dark for 10 min to fully stain n-hexadecane with NR. Finally, observation was performed under an optical microscope equipped with a mercury lamp and filter.

(2) Calcofluor White (CWS) staining of RCNC. First, 200 µL of 1 g/L RCNC-stabilized Pickering emulsion was dispersed in 2 mL 50 mmol/L NaCl aqueous solution. Then, 20 µL CWS was added, and allowed to stand in the dark for 10 min to fully stain RCNC with CWS. Finally, observation was performed under an optical microscope equipped with a mercury lamp and filter.

(3) Double staining of NR and CWS. Under the same conditions, 20 µL of NR and CWS staining solutions were sequentially added dropwise to the emulsion dispersion, and allowed to stand in the dark for 10 min to fully stain n-hexadecane and RCNC with fluorescent dyes. Finally, observation was performed under an optical microscope equipped with a mercury lamp and filter.

2.7 Photodegradation rate characterization

First, the ZnO@RCNC-stabilized Pickering emulsion was transferred to an aluminum foil-covered petri dish with a diameter of 7.5 cm. Then, the petri dish was placed about 15 cm below a light source (xenon lamp, PLS-SXE300) for irradiation test. Every 20 min, 500 µL of NR-stained n-hexadecane sample was taken, mixed uniformly with 2 mL unstained n-hexadecane in a quartz cuvette, and the NR content after different irradiation times was determined by ultraviolet-visible spectrophotometer (UV-vis, UV-2600), using the absorbance of NR at 492 nm as the characteristic peak. During the irradiation test, except for sampling, the petri dish was covered with a quartz plate to prevent water evaporation, and the emulsion was magnetically stirred at 200 r/min throughout.

The degradation rate was expressed as relative content, as shown in formula (1):

$$C = C_t / C_0 \times 100\% \quad (1)$$

Where: C is the relative content; C_t is the absorption intensity of NR after irradiation for t min; C_0 is the absorption intensity of NR at 0 min irradiation.

Low-temperature centrifugation demulsification was used to separate NR-stained n-hexadecane after different

illumination times from the sampled emulsion: since the melting point of n-hexadecane is 18 °C, the emulsion sampled at equal time intervals was centrifuged at 10000 r/min (Eppendorf 5810 R) for 10 min at 10 °C, then heated until the solidified stained n-hexadecane was completely melted, and then 500 μL was taken for UV-vis test.

3 Results and analysis

3.1 RCNC characterization

NaOH/urea/water system has been widely proven to be an effective solvent for dissolving cellulose[9,16]. In the pre-cooled NaOH/urea/water system, NaOH hydrate and cellulose molecular chains form stable hydrogen bond ligands at low temperature, and sheath-like urea hydrate as a shell wraps the NaOH-hydrogen bond-cellulose ligand to form an inclusion complex (IC) channel to prevent the association between cellulose molecules, thereby causing cellulose dissolution[17-18].

Figure 1(a) shows that with the batch addition of anhydrous ethanol, the molecular weight of RCNC samples gradually decreased from 36 kDa to 9 kDa. According to the molecular weight, the obtained RCNC were named: RCNC-36, RCNC-25, RCNC-15, RCNC-11, RCNC-10, RCNC-9. The inset of Figure 1(a) shows the D_M of RCNC. It can be seen that RCNC-36 and RCNC-25 have higher D_M, indicating that these two regenerated celluloses have a wide molecular weight distribution, large molecular weight differences, and poor sample uniformity. Anhydrous ethanol enhances the inter/intra-molecular hydrogen bonds of cellulose by destroying the sheath-like urea coating complex, causing it to precipitate from the solvent. The continuous precipitation of RCNC with decreasing molecular weight from the remaining solution may be because the smaller the cellulose molecular weight, the greater the degree of coating by urea coating complex, and the stronger the hydrogen bond between cellulose molecules and NaOH/urea/water system, so higher concentration of anhydrous ethanol is needed to destroy the sheath-like urea hydrate through competitive hydrogen bonding, thereby precipitating low-molecular-weight cellulose from the solution. Therefore, by gradually adding anti-solvent (anhydrous ethanol) to the cellulose solution, polysaccharide components with gradually decreasing molecular weight can be obtained.

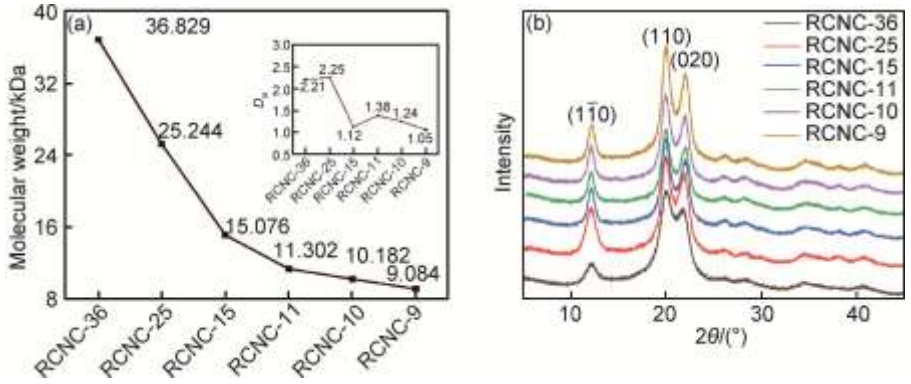

Figure 1 Mw of RCNC, inset: DM of RCNC (a), and XRD patterns of the prepared RCNC (b)

The crystal configuration and amphiphilicity of cellulose-based emulsion stabilizers are important factors affecting their emulsifying performance. Figure 1(b) shows the XRD patterns of RCNC samples. It can be seen from Figure 1(b) that the XRD characteristic peaks of RCNC-36 to RCNC-9 basically remain consistent, all showing three characteristic peaks at 2θ = 12.2°, 20.0°, 22.2° corresponding to the (1$\overline{1}$0), (110), (020) crystal planes of cellulose II[19]. In the initial stage of cellulose regeneration, pyranoside rings first stack to form molecular layers through hydrophobic interaction, and then the molecular layers arrange to form Na-IV cellulose microcrystals through hydrogen bonds[20]. When Na-IV cellulose transforms into cellulose II, the (1$\overline{1}$0) crystal plane spacing decreases[21], indicating that water molecules are located between the stacking of hydrophobic crystal planes in the [110] direction. The (110) plane of cellulose II is a hydrophobic plane, so cellulose II is amphiphilic (the crystal model is shown in Figure 2). This indicates that the obtained RCNC

is amphiphilic and can be used as a Pickering emulsion stabilizer.

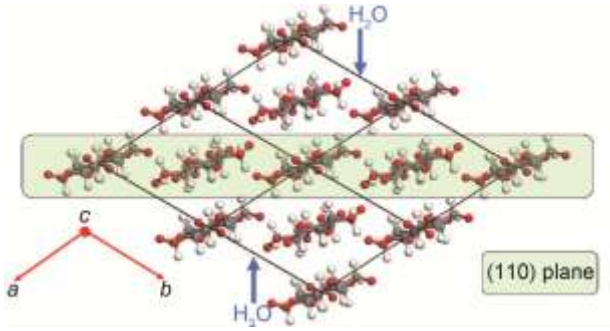

Figure 2 Schematic diagram of hydrophobic crystal surface of cellulose II

Figure 3 shows TEM images of RCNC-n. Most samples in RCNC-36 and RCNC-25 have larger sizes due to their higher molecular weights (Figure 3(a), (b)). However, the sizes of the two are not uniform. During the experiment, some agglomerated RCNC with sizes of several microns were also observed. Figure 3(b) shows the local area of agglomerated RCNC in RCNC-25. The reason for the non-uniform size of these two RCNC samples is their wide molecular weight distribution (Figure 1(a)), leading to large size differences. When the sample molecular weight is less than or equal to 15 kDa, its molecular weight and size tend to be stable. As the sample molecular weight further decreases, the corresponding size of RCNC decreases (Figure 3(c)~(f)).

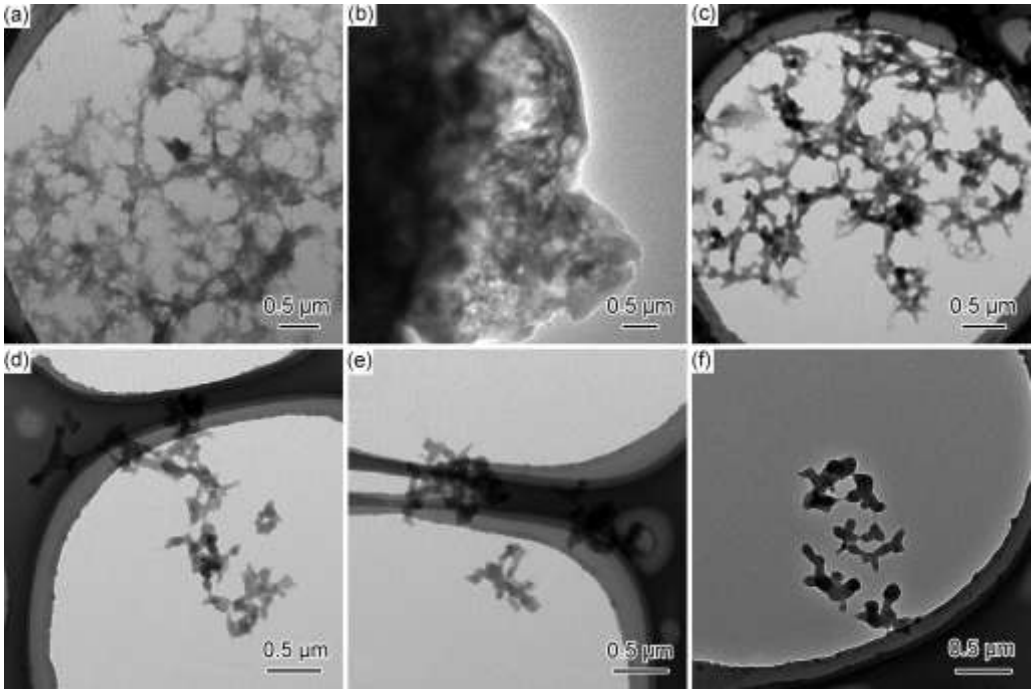

Figure 3 TEM images of RCNC-n (a) RCNC-36; (b) RCNC-25; (c) RCNC-15; (d) RCNC-11; (e) RCNC-10 (f) RCNC-9

3.2 Characterization of Pickering emulsion stability of RCNC-n

Figure 4 shows photos of the O/W Pickering emulsion stabilized by the obtained RCNC-n. It can be seen from Figure 4 that the emulsion stabilized by RCNC-15 has the thickest emulsification layer, while the emulsification layers of RCNC-36 and RCNC-25 are thinner, about half of that of RCNC-15, indicating that RCNC-36 and RCNC-25 have the worst emulsifying performance. After the molecular weight distribution stabilizes, RCNC-15 has the best emulsifying effect, and the emulsifying effect of other samples decreases with decreasing molecular weight.

It was found in the experiment that when the content of RCNC-n was less than 2 g/L (Table 1), the emulsions corresponding to RCNC-36 and RCNC-25 had poor stability and broke during the transfer to microscopic observation, so their droplet sizes could not be measured, which corresponds to the thinnest emulsification layer of the two in Figure 4.

Figure 4 Optical image of an O/W Pickering emulsion prepared with 2 g/L RCNC-n

Table 1 Droplet diameter of RCNC-n-stabilized O/W Pickering emulsions at different loadings after 24 h and 14 d

Sample	0.5 g/L (24 h / 14 d)	1 g/L (24 h / 14 d)	2 g/L (24 h / 14 d)	4 g/L (24 h / 14 d)
RCNC-36	x/x	611/x	119.0/123.8	57.2/65.9
RCNC-25	x/x	x/x	180.9/199.0	90.8/115.1
RCNC-15	65.1/80.7	28.1/28.3	13.1/13.2	7.9/7.7
RCNC-11	74.3/101.9	30.2/38.5	15.5/15.8	8.5/8.6
RCNC-10	78.1/110.5	42.8/42.9	27.7/27.7	14.2/14.1
RCNC-9	85.2/121.7	56.7/60.5	28.4/28.8	15.1/15.0

Due to the wide molecular weight distribution and poor emulsifying performance of RCNC-36 and With the exception of RCNC-25, the size-fractionated RCNC series (RCNC-15 through RCNC-9), characterized by uniform molecular weights and dimensions, was exploited to systematically investigate the effect of RCNC molecular weight and size on emulsion stability. Optical micrographs of emulsions stabilized by RCNC-15 to RCNC-9 at varying concentrations are compiled in Figure 5. The images reveal a clear inverse correlation between RCNC-n concentration (from RCNC-15 to RCNC-9) and droplet diameter. At the minimum dosage examined (0.5 g L^{-1}), a pronounced increase in droplet size was observed after 14 days, indicative of coalescence. Conversely, emulsions formulated at higher RCNC-n concentrations exhibited negligible dimensional changes over the identical storage duration.

To compare the change of droplet size of emulsions with different contents of RCNC-n (RCNC-15~9), the measurement results of droplet size after 14 days of storage are shown in Figure 6. It can be seen from Figure 6 that when the content of RCNC-n was less than or equal to 1 g/L, the droplets of the prepared emulsions all showed an increase in size, and the emulsion with 0.5 g/L RCNC-n had the worst stability. This is because for most Pickering emulsion systems, when the colloidal particle content is low, due to the limited number of available colloidal particles, the interface area that can be stabilized is small, resulting in larger emulsion droplet size, and the oil phase surface cannot be completely covered, so the emulsion stability is poor and prone to coalescence[22]. The higher the content of RCNC-n used, the smaller the emulsion droplet size, because when the oil phase volume is the same, the smaller the droplet size, the larger the specific surface area formed, so higher content of colloidal particles is needed to stabilize the larger specific surface area[23]. It can also be seen from Figure 6 that when the content of RCNC-n was constant, as the molecular weight of RCNC-n decreased, the size of the stabilized emulsion droplets increased and the emulsion performance became worse, which is opposite to the currently common phenomenon[24-25].

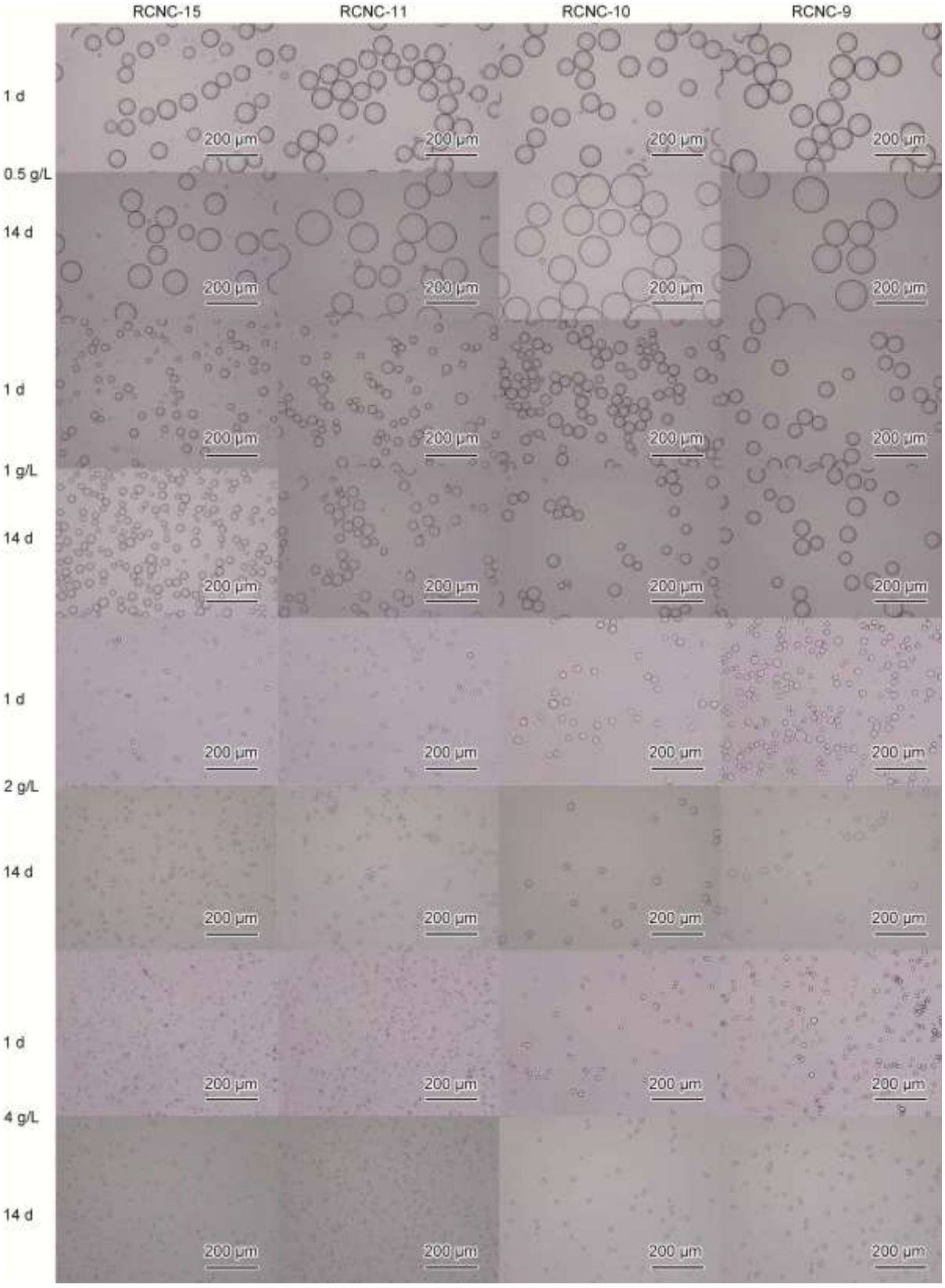

Figure 5 OM images of O/W Pickering emulsion stabilized by RCNC-n

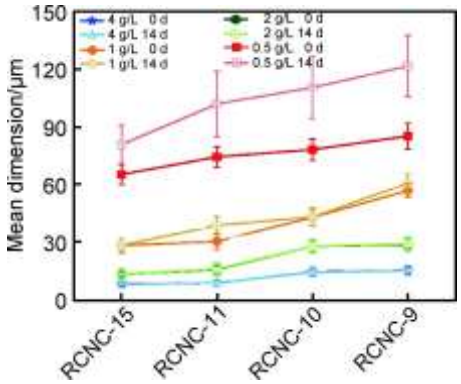

Figure 6 Droplet sizes variation tendency of the O/W Pickering emulsion stabilized by the RCNC-n samples with different concentrations before and after 14 d storage

As illustrated in Figure 7, RCNC‑10 assembled into a stable, homogeneous interfacial film at the oil–water boundary[14,26–27]. Soft particles can bend on the oil droplet surface to produce strong effective interfacial anchoring and dense interfacial coverage[14,28]. In addition, particles with anisotropy have stronger interfacial packing and can cover a larger interfacial area[29]. Therefore, RCNC-15 has relatively good emulsifying performance, probably due to its good bending deformation ability and higher anisotropy, enabling it to bend on the oil droplet surface and produce strong effective interfacial anchoring. As the molecular weight and size decrease, the rigidity of RCNC-11 to RCNC-9 gradually increases, and their bending degree at the two-phase interface decreases, resulting in a decrease in effective interfacial anchoring and coverage at the two-phase interface, so their interfacial barrier ability decreases, leading to a gradual decrease in the corresponding emulsion stability and obvious emulsion coalescence phenomenon (Figure 5).

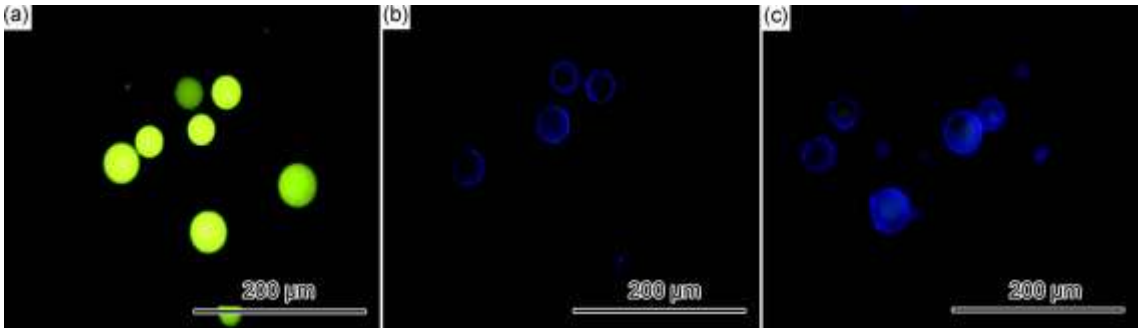

Figure 7 Fluorescence images of 1 g/L RCNC-10 Pickering emulsion: (a) NR–oil; (b) CWS–RCNC; (c) merged

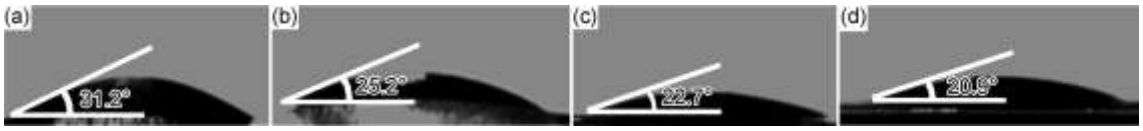

Figure 8 Contact angle images of RCNC-n (a) RCNC-15; (b) RCNC-11; (c) RCNC-10; (d) RCNC-9

The ability of colloidal particles to hinder emulsion coalescence can be evaluated by the strength of adsorption free energy of colloidal particles at the two-phase interface. The mechanism of Pickering emulsion stabilized by non-spherical colloidal particles is more complicated and difficult to describe quantitatively[14]. For spherical particles, the adsorption free energy is proportional to the square of the spherical radius, as shown in formula (2):

$$\Delta E = \pi R^2 \gamma (1-|\cos\theta|)^2 \qquad (2)$$

Where: ΔE is the adsorption free energy; R and γ represent the radius of colloidal particles and interfacial tension respectively; θ is the contact angle. The wettability of Pickering emulsion stabilizer is also an important parameter affecting emulsion stability[14,23]. Figure 8 shows photos of static contact angles of RCNC-15 to RCNC-9. It can be seen from Figure 8 that RCNC-15 self-supporting film has the largest hydrophobicity, and the contact angle of water droplets on RCNC-n self-supporting film gradually decreases with the decrease of molecular weight. It is not difficult to conclude from formula (2) that the larger the static hydrophobic angle, the greater the adsorption free energy at the two-phase interface, so RCNC-15 can form effective interfacial anchoring at the two-phase interface, and its stabilized emulsion has the best stability and the emulsion droplets are not easy to coalesce.

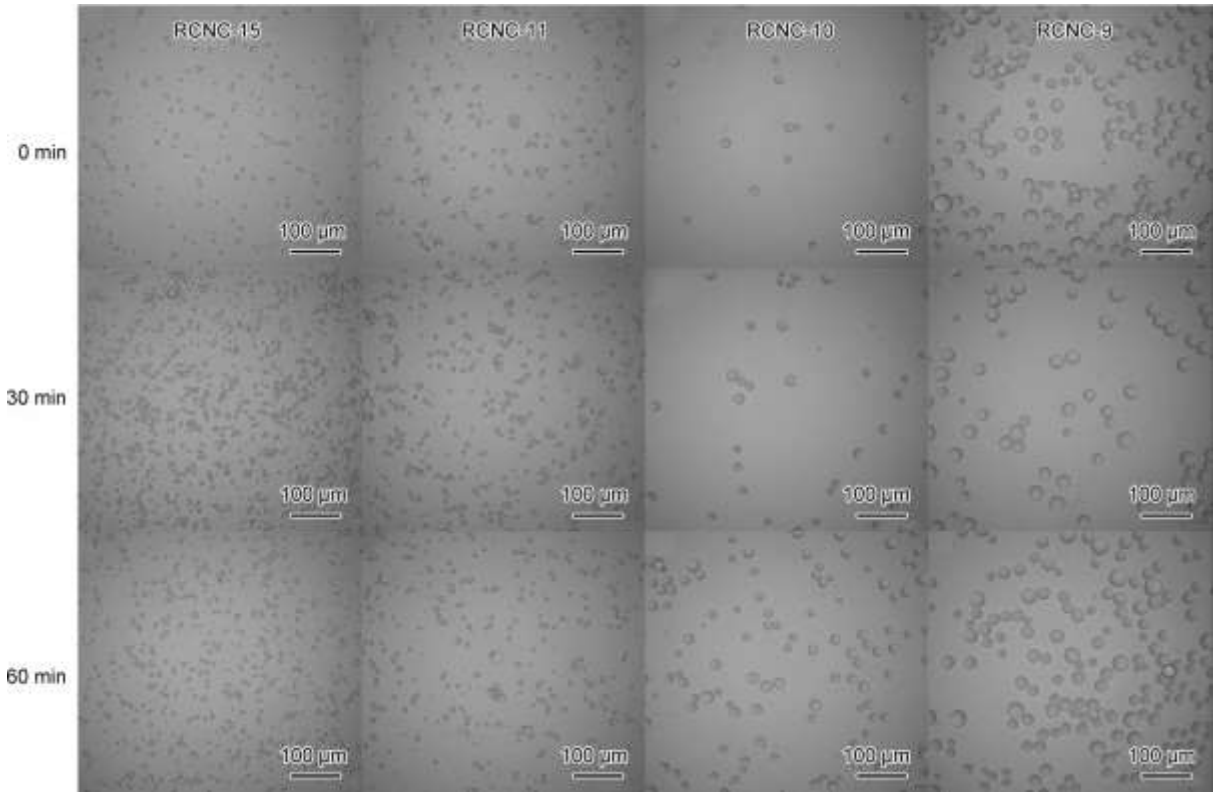

Figure 9 OM images of O/W Pickering emulsion droplets stabilized by RCNC-n at a concentration of 2 g/L and after standing for 6 months and undergone different centrifuge time (0, 30, 60 min) under 10000 r/min

In addition to droplet coalescence caused by rupture of droplet covering layer, Ostwald ripening caused by Laplace pressure difference between droplets is also an important process in the destabilization process[26]. The Young-Laplace equation (Y-L equation) is shown in formula (3):

$$\Delta P = \gamma(1/R_1 + 1/R_2) \qquad (3)$$

Where: ΔP is the Laplace pressure of the droplet; γ is the interfacial tension; R_1 and R_2 are the curvature radii in the latitude and longitude directions of the small sphere respectively[30]. It can be approximately considered that the emulsion droplets are spherical, so the Y-L equation can be rewritten as: $\Delta P = 2\gamma/R$. The ΔP of the droplet is proportional to γ and inversely proportional to R. Since surface tension is a function of droplet size: that is, as the size decreases, the surface tension decreases[31]. Therefore, when the tension difference between droplets of different sizes and the balanced capillary pressure difference reach a quasi-steady state, the droplet size will tend to a constant value, that is, with a smaller standard deviation. Therefore, compared with other RCNC-n (RCNC-11~9), the emulsion droplets stabilized by RCNC-15 have the smallest standard deviation of size, that is, a smaller standard deviation (Figure 6), so the ΔP between droplets is smaller, Ostwald ripening is not obvious,

and thus it shows relatively best emulsion stability. However, the molecular weight distribution of RCNC-36 and RCNC-25 is wide and the size is not uniform, resulting in non-uniform emulsion droplet size stabilized by them, serious Ostwald ripening phenomenon, poor emulsion stability, and even phase separation.

The emulsion stabilized by RCNC-n with a content of 2 g/L was selected, and after 6 months of storage, the centrifugal stability of these emulsions was further tested by centrifugation loading. Figure 9 shows optical microscope photos of the emulsion after different centrifugation times. The droplet sizes of Pickering emulsions stabilized by RCNC-15~9 show no significant change after different centrifugation times. The centrifugation results show that the Pickering emulsions stabilized by 2 g/L RCNC-15~9 have excellent time stability and centrifugal stability.

The temperature stability of Pickering emulsions stabilized by RCNC-n was further tested by storing at different temperatures. Figure 10 shows optical microscope photos of Pickering emulsions stabilized by 2 g/L RCNC-15~9 after storing at room temperature for 6 months and then at different temperatures for 24 h [32]. Figure 10 further shows that the effective interfacial anchoring generated by RCNC-n at the two-phase interface gives it good thermal stability, indicating that the material can adapt to various temperature environments.

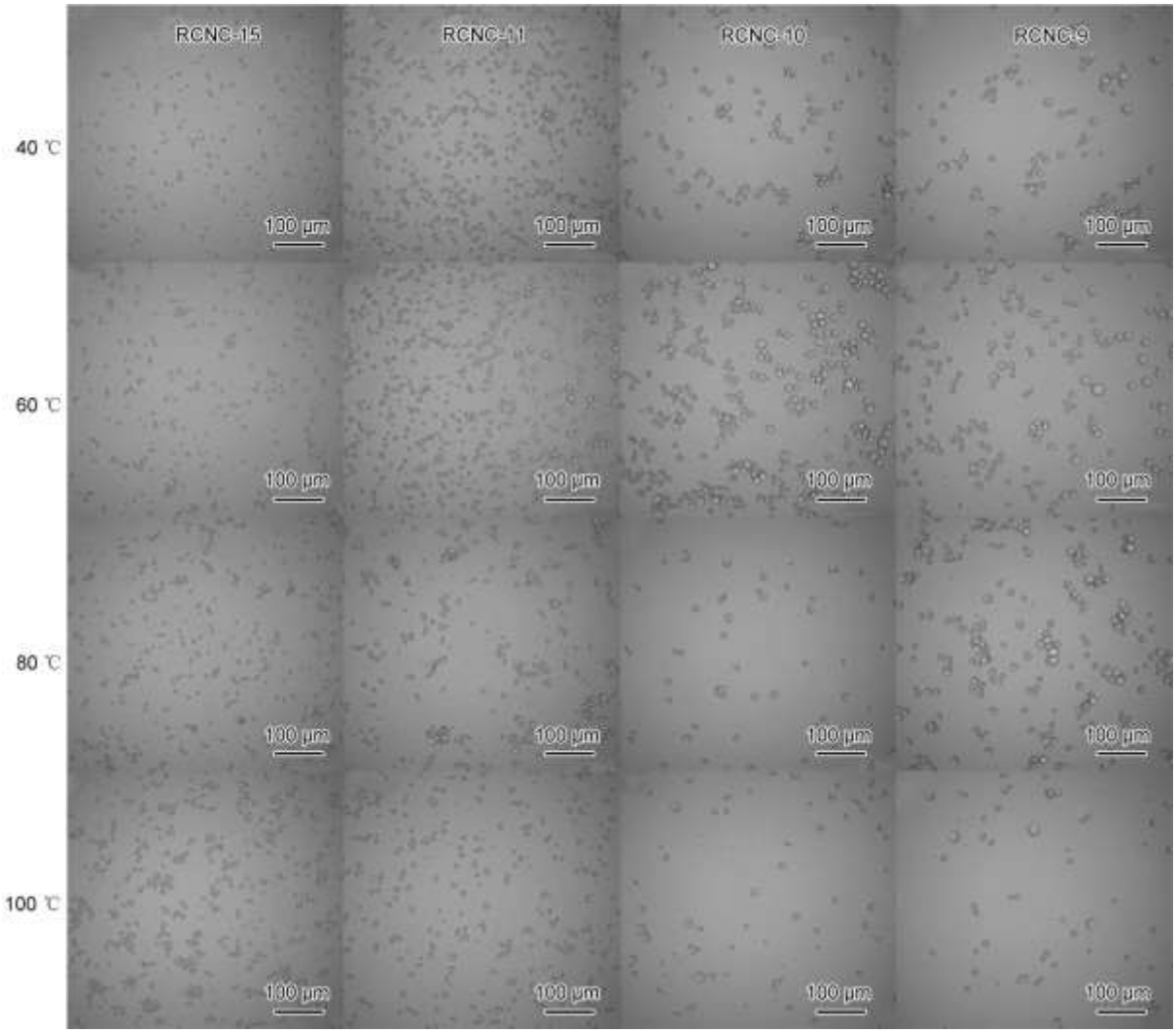

Figure 10 OM images of Pickering emulsion stabilized by RCNC-n with a concentration of 2 g/L after standing for 6 months and keeping at 40, 60, 80, 100 ℃ for 24 h， respectively

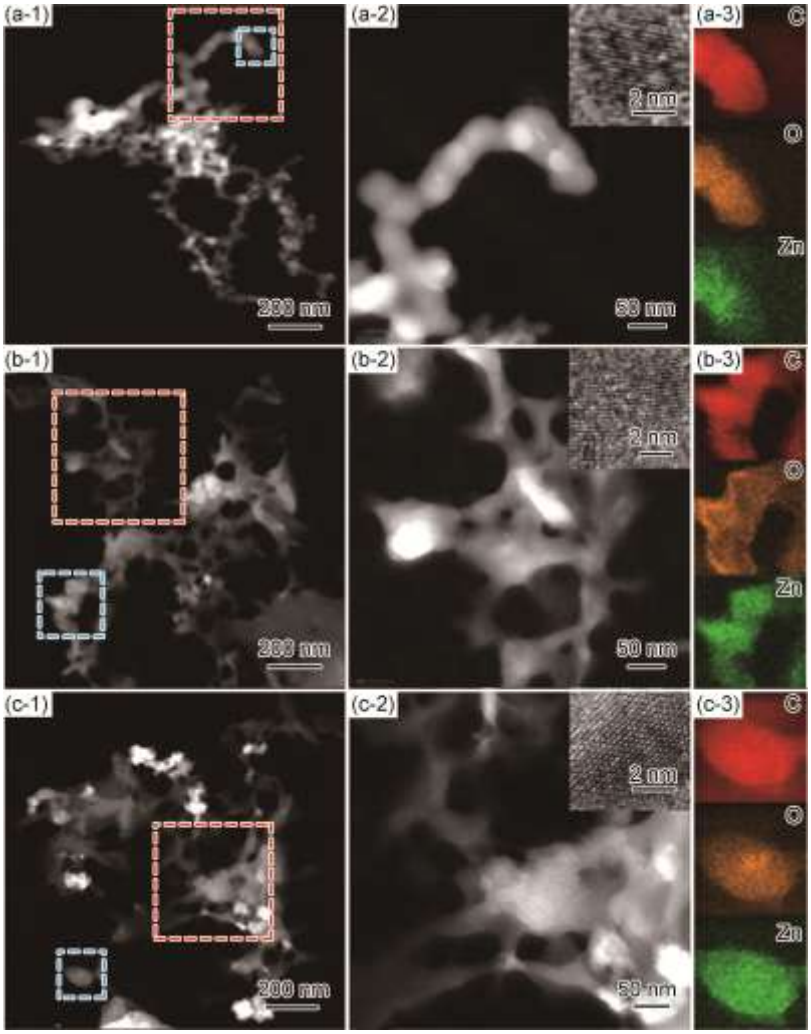

Figure 11 HAADF-STEM image (1), magnified view of the red-box area (2), and the EDS mapping of the blue-box area (3) of samples (a) ZnO@RCNC-15_1:2; (b) ZnO@RCNC-15_2:2; (c)ZnO@RCNC-15_3:2

3.3 Photodegradation performance characterization of ZnO@RCNC-15_x:2 composite

Compared with inorganic nanoparticles, another advantage of regenerated cellulose nanomaterials as emulsion stabilizers is that they have abundant modifiable functional groups on their surface. On the one hand, their emulsifying performance can be regulated by chemical modification; on the other hand, other nanoparticles (such as catalysts) can be introduced on their surface to carry out emulsion-assisted reactions and improve chemical reaction efficiency.

Photodegradation of organic dyes usually occurs at the interface between the photocatalyst and pollutants[33]. However, due to large specific surface area and high surface energy, zinc oxide nanoparticles (ZnONPs) tend to agglomerate[34]. In addition, exposed ZnONPs have strong hydrophilicity, making the Pickering emulsion stabilized by ZnONPs poor performance[35]. Therefore, it is difficult to effectively use ZnONPs alone to degrade oil-soluble organic dyes. In order to improve the dispersion and utilization of ZnO NPs, ZnONPs were grown in situ on the surface of RCNC-15 with the best emulsifying performance, and ZnO@RCNC-15_x:2 composites with different mass ratios were prepared for photo-degradation test of NR model reaction.

It can be observed from Figure 11 that with the increase of zinc nitrate dosage, the number of ZnONPs (white bright spots) grown in situ on RCNC-15 gradually increases. According to HAADF-STEM photos and corresponding EDS maps, it can be seen that ZnONPs are evenly distributed on the surface of RCNC-15. ICP-MS characterization

of the ZnO content on its surface shows that the ZnO contents in ZnO@RCNC-15_1:2, ZnO@RCNC-15_2:2, ZnO@RCNC-15_3:2 are 0.27%, 0.47%, 0.51% respectively. However, with the increase of ZnO content, aggregation of ZnONPs begins to appear on the surface of ZnO@RCNC-15_3:2 (Figure 11(c)).

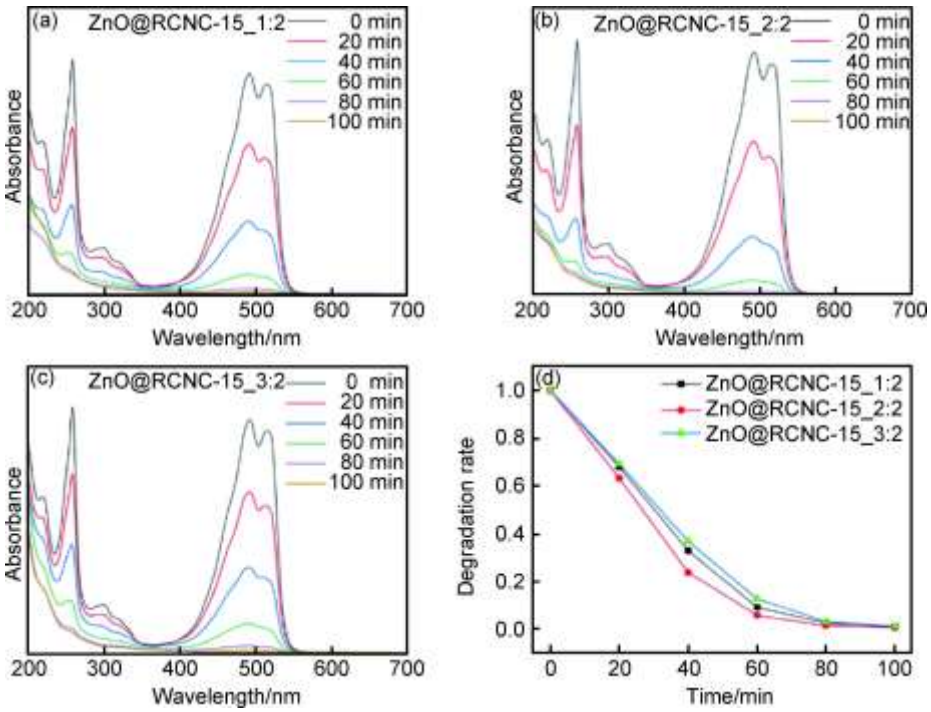

Figure 12 UV-vis spectra of NR undergone 0, 20, 40, 60, 80, and 100 min (a)-(c), and photocatalytic degradation rate versus time of ZnO@RCNC-15_x:2 (d)

It can be seen from Figures 12(a)~(c) that with the increase of irradiation time, the light absorption intensity of NR significantly decreases, indicating that NR is gradually degraded. Figure 12(d) shows the relationship between photocatalytic degradation rate and time of ZnO@RCNC-15_x:2 composites. After calculation, after 80 min of irradiation, the degradation rates of NR by ZnO@RCNC-15_1:2, ZnO@RCNC-15_2:2, ZnO@RCNC-15_3:2 are 97.5%, 98.6%, 97.0% respectively. After 100 min of irradiation, the degradation rates reach 99.2%, 99.5%, 98.9% respectively. Among them, ZnO@RCNC-15_2:2 has the highest degradation efficiency.

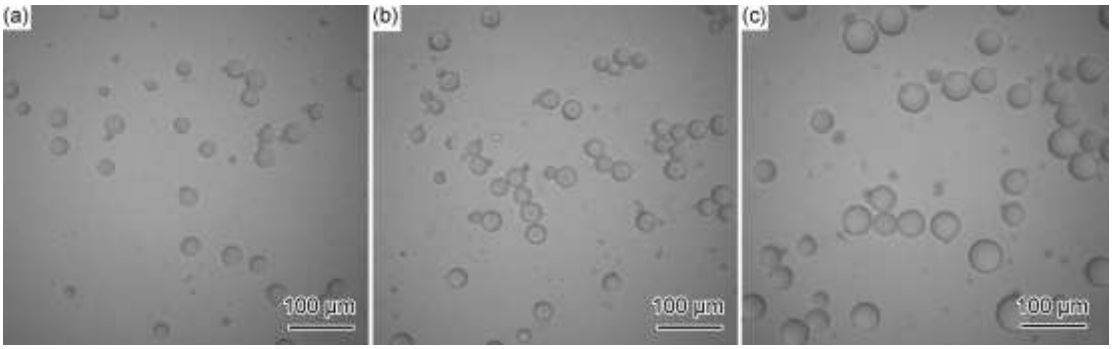

Figure 13 OM images of Pickering emulsion stabilized by ZnO@RCNC-15_1:2(a), ZnO@RCNC-15_2:2(b), and ZnO@RCNC-15_3:2 (c)

According to ICP-MS results, the ZnO content of ZnO@RCNC-15_2:2 (0.47%) is higher than that of ZnO@RCNC-15_1:2 (0.27%), so its photodegradation rate is faster than that of ZnO@RCNC-15_1:2. However, due to the strong hydrophilicity of ZnO, the emulsifying performance of RCNC-15 with in situ grown ZnONPs slightly decreases. As shown in Figure 13, the droplet sizes of emulsions stabilized by ZnO@RCNC-15_1:2 and

ZnO@RCNC-15_2:2 are not much different, but compared with the emulsion stabilized by single RCNC-15 with the same content (2 g/L) (Figure 5), its droplet size slightly increases. This is mainly because the hydrophobicity of RCNC-15 with in situ grown strongly hydrophilic ZnONPs decreases, resulting in increased emulsion size. In addition, it can be observed from Figure 13 that the droplet size of emulsion stabilized by ZnO@RCNC-15_3:2 significantly increases, which is mainly because at this ZnO NPs content (0.51%), ZnO NPs agglomeration appears on the surface of RCNC-15 (Figure 11(c)), further leading to a decrease in its hydrophobicity. Due to the increase in droplet size of emulsion stabilized by ZnO@RCNC-15_3:2, the oil/water interface area decreases, thereby reducing the effective reaction area between ZnONPs and NR. In addition, due to the increase in droplet size, the NR content in a single droplet increases, further leading to a decrease in photocatalytic rate.

In summary, when the droplet size of Pickering emulsion stabilized by ZnO@RCNC-15 composite remains unchanged (i.e., ZnO@RCNC-15_1:2 and ZnO@RCNC-15_2:2), the increase of in situ grown ZnONPs content can effectively increase the photodegradation rate. However, when the content of ZnONPs increases to cause a significant increase in the droplet size of Pickering emulsion stabilized by it (i.e., ZnO@RCNC-15_3:2), although it has a higher ZnONPs content, its photodegradation rate decreases significantly.

4 Conclusions

(1) A series of cellulose II RCNC materials with gradually decreasing average molecular weight and size were obtained by an improved multi-step precipitation method. When the molecular weight of RCNC was 36 kDa and 25 kDa, its molecular weight distribution was wide and the morphology was not uniform; when the molecular weight of RCNC was less than or equal to 15 kDa, its molecular weight distribution and size tended to be stable, and the corresponding size decreased with the decrease of molecular weight.

(2) RCNC-15, averaging 15 kDa in molecular weight, exhibited the most favourable emulsifying behaviour, affording the finest droplet dimensions and the greatest stability at minimal stabiliser loadings. Its uniform size, good soft deformability and high interfacial adsorption free energy enable it to produce effective interfacial anchoring at the two-phase interface. When the content of RCNC is greater than 2 g/L, the emulsions stabilized by RCNC-15 to RCNC-9 samples all have good time, mechanical and temperature stability.

(3) The excellent emulsifying performance of RCNC-15 sample enables it to be used as an emulsion reaction carrier, and in situ growth of ZnONPs achieves efficient emulsion-assisted photo-degradation of Nile red. At the same time, it was also found that on the premise that the emulsion droplet size is constant, the increase of ZnONPs content helps to increase the photodegradation rate. However, further increasing the content of ZnONPs will affect the hydrophobicity of RC emulsion stabilizer, resulting in increased emulsion droplet size and slowed photodegradation rate.

References

[1] LANGAN P, NISHIYAMA Y, CHANZY H. X-ray structure of mercerized cellulose II at 1 Å resolution[J]. Biomacromolecules, 2001, 2(2): 410-416.
[2] MOON R J, MARTINI A, NAIRN J, et al. Cellulose nanomaterials review: structure, properties and nanocomposites[J]. Chemical Society Reviews, 2011, 40(7): 3941.
[3] ZHENG Y, FU Z, LI D, et al. Effects of ball milling processes on the microstructure and rheological properties of microcrystalline cellulose as a sustainable polymer additive[J]. Materials, 2018, 11(7): 1057.
[4] MANDAL A, CHAKRABARTY D. Isolation of nanocellulose from waste sugarcane bagasse (SCB) and its characterization[J]. Carbohydrate Polymers, 2011, 86(3): 1291-1299.
[5] SHANG Z, AN X, SETA F T, et al. Improving dispersion stability of hydrochloric acid hydrolyzed cellulose nano-crystals[J]. Carbohydrate Polymers, 2019, 222: 115037.
[6] TAO P, ZHANG Y, WU Z, et al. Enzymatic pretreatment for cellulose nanofibrils isolation from bagasse pulp: transition of cellulose crystal structure[J]. Carbohydrate Polymers, 2019, 214: 1-7.
[7] NECHYPORCHUK O, BELGACEM M N, BRAS J. Production of cellulose nanofibrils: a review of recent advances[J]. Industrial Crops and Products, 2016, 93: 2-25.
[8] MEDRONHO B, ROMANO A, MIGUEL M G, et al. Rationalizing cellulose (in)solubility: reviewing basic

physicochemical aspects and role of hydrophobic interactions[J]. Cellulose, 2012, 19(3): 581-587.
[9] CAI J, ZHANG L. Rapid dissolution of cellulose in LiOH/urea and NaOH/urea aqueous solutions[J]. Macromolecular Bioscience, 2005, 5(6): 539-548.
[10] SWATLOSKI R P, SPEAR S K, HOLBREY J D, et al. Dissolution of cellulose with ionic liquids[J]. Journal of the American Chemical Society, 2002, 124(18): 4974-4975.
[11] KUO C H, LEE C K. Enhancement of enzymatic saccharification of cellulose by cellulose dissolution pretreatments[J]. Carbohydrate Polymers, 2009, 77(1): 41-46.
[12] RAMSDEN W. Separation of solids in the surface-layers of solutions and 'suspensions' (observations on surface-membranes, bubbles, emulsions, and mechanical coagulation): preliminary account[J]. Proceedings of the Royal Society of London, 1903, 72: 156-164.
[13] PICKERING S U. CXCVI.—Emulsions[J]. Journal of the Chemical Society, Transactions, 1907, 91: 2001-2021.
[14] ALBERT C, BELADJINE M, TSAPIS N, et al. Pickering emulsions: preparation processes, key parameters governing their properties and potential for pharmaceutical applications[J]. Journal of Controlled Release, 2019, 309: 302-332.
[15] OGAWA Y, PUTAUX J L. Transmission electron microscopy of cellulose. Part 2: technical and practical aspects[J]. Cellulose, 2019, 26(1): 17-34.
[16] LUE A, ZHANG L. Advances in aqueous cellulose solvents[M]//Cellulose solvents: for analysis, shaping and chemical modification. Washington, DC: American Chemical Society, 2010: 67-89.
[17] WANG S, LU A, ZHANG L. Recent advances in regenerated cellulose materials[J]. Progress in Polymer Science, 2016, 53: 169-206.
[18] CAI J, ZHANG L, CHANG C, et al. Hydrogen-bond-induced inclusion complex in aqueous cellulose/LiOH/urea solution at low temperature[J]. ChemPhysChem, 2007, 8(10): 1572-1579.
[19] SÈBE G, HAM-PICHAVANT F, IBARBOURE E, et al. Supramolecular structure characterization of cellulose II nanowhiskers produced by acid hydrolysis of cellulose I substrates[J]. Biomacromolecules, 2012, 13(2): 570-578.
[20] ISOBE N, KIMURA S, WADA M, et al. Mechanism of cellulose gelation from aqueous alkali-urea solution[J]. Carbohydrate Polymers, 2012, 89(4): 1298-1300.
[21] KOBAYASHI K, KIMURA S, TOGAWA E, et al. Crystal transition from Na-cellulose IV to cellulose II monitored using synchrotron X-ray diffraction[J]. Carbohydrate Polymers, 2011, 83(2): 483-488.
[22] JUÁREZ J A, WHITBY C P. Oil-in-water Pickering emulsion destabilisation at low particle concentrations[J]. Journal of Colloid and Interface Science, 2012, 368(1): 319-325.
[23] WU J, MA G H. Recent studies of Pickering emulsions: particles make the difference[J]. Small, 2016, 12(34): 4633-4648.
[24] DICKINSON E. Use of nanoparticles and microparticles in the formation and stabilization of food emulsions[J]. Trends in Food Science & Technology, 2012, 24(1): 4-12.
[25] BINKS B P, LUMSDON S O. Pickering emulsions stabilized by monodisperse latex particles: effects of particle size[J]. Langmuir, 2001, 17(15): 4540-4547.
[26] DESHMUKH O S, VAN DEN ENDE D, STUART M C, et al. Hard and soft colloids at fluid interfaces: adsorption, interactions, assembly & rheology[J]. Advances in Colloid and Interface Science, 2015, 222: 215-227.
[27] SCHMIDT S, LIU T, RÜTTEN S, et al. Influence of microgel architecture and oil polarity on stabilization of emulsions by stimuli-sensitive core-shell poly(N-isopropylacrylamide-co-methacrylic acid) microgels: Pickering versus Pickering behavior?[J]. Langmuir, 2011, 27(16): 9801-9806.
[28] DESTRIBATS M, LAPEYRE V, WOLFS M, et al. Soft microgels as Pickering emulsion stabilisers: role of particle deformability[J]. Soft Matter, 2011, 7(17): 7689.
[29] MADIVALA B, VANDEBRIL S, FRANSAER J, et al. Exploiting particle shape in solid stabilized emulsions[J]. Soft Matter, 2009, 5(8): 1717.
[30] VAFAEI S, WEN D. Modification of the Young-Laplace equation and prediction of bubble interface in the presence of nanoparticles[J]. Advances in Colloid and Interface Science, 2015, 225: 1-15.
[31] ASHBY N P, BINKS B P. Pickering emulsions stabilised by Laponite clay particles[J]. Physical Chemistry Chemical Physics, 2000, 2(24): 5640-5646.
[32] SHARMA T, KUMAR G S, CHON B H, et al. Thermal stability of oil-in-water Pickering emulsion in the presence of nanoparticle, surfactant, and polymer[J]. Journal of Industrial and Engineering Chemistry, 2015, 22: 324-334.
[33] LEFATSHE K, MUIVA C M, KEBAABETSWE L P. Extraction of nanocellulose and in-situ casting of ZnO/cellulose nanocomposite with enhanced photocatalytic and antibacterial activity[J]. Carbohydrate

Polymers, 2017, 164: 301-308.
[34] AZIZI S, AHMAD M, MAHDAVI M, et al. Preparation, characterization, and antimicrobial activities of ZnO nanoparticles/cellulose nanocrystal nanocomposites[J]. BioResources, 2013, 8(2): 1841-1851.
[35] CIONTI C, VAVASSORI G, PARGOLETTI E, et al. One-step, highly stable Pickering emulsions stabilized by ZnO: tuning emulsion stability by in situ functionalization[J]. Journal of Colloid and Interface Science, 2022, 628: 82-89.